**Ocean Science
Discussions**

Transport of warm upper circumpolar deep water onto the Western Antarctic Peninsula Continental Shelf

D. G. Martinson

Division of Ocean and Climate Physics, Lamont-Doherty Earth Observatory of Columbia University, 61 Route 9W, Palisades, NY, 10964, USA

Department of Earth and Environmental Sciences, Columbia University, New York, NY, USA

Correspondence to: D. G. Martinson (dgm@ldeo.columbia.edu)

Discussion Paper | Discussion Paper | Discussion Paper | Discussion Paper

OSD

8, 2479–2502, 2011

Transport of warm upper circumpolar deep water

D. G. Martinson

Title Page

Abstract | Introduction

Conclusions | References

Tables | Figures

|◀ | ▶|

◀ | ▶

Back | Close

Full Screen / Esc

Printer-friendly Version

Interactive Discussion

Abstract

Five thermistor-moorings were placed on the continental shelf of the Western Antarctic Peninsula (between 2007 and 2010) in an effort to identify the mechanism(s) responsible for delivering warm Upper Circumpolar Deep Water (UCDW) onto the broad con-
5 tinental shelf from the Antarctic Circumpolar Current (ACC) flowing over the adjacent continental slope. Historically, four mechanisms have been suggested (or assumed): (1) eddies shed from the ACC, (2) flow into the cross-shelf-cutting canyons with overflow onto the nominal shelf, (3) general upwelling, and (4) episodic sweeping of ACC meanders over the shelf. The mooring array showed that for the years of deployment,
10 the dominant mechanism is eddies; upwelling may also contribute but to an unknown extent. Mechanisms 2 and 4 played no role, though the canyons have been shown previously to channel UCDW across the shelf into Marguerite Bay.

1   Introduction

The Antarctic Peninsula (AP) is undergoing extraordinary climate change – Earth's
15 most extreme *winter* atmospheric warming, and severe sea ice and glacial ice loss with 87 % of the marine glaciers in retreat (Cook et al., 2005). Vaughan (2005) notes that the winter warming points to the ocean for the source of heat (the obvious source of heat in the region in winter, when there is no real radiative forcing at the polar circle, and no warm air masses of any substance advecting through). Martinson et al. (2008)
20 documented an increase in ocean heat content along the west Antarctic Peninsula (WAP) margin. In order to appreciate the long-term implications of this ocean heat we must understand the mechanisms delivering warm water onto the continental shelf and the ultimate source of heat. These needs motivated the deployment of the International Polar Year Synoptic Antarctic Slope-Shelf Interaction (IPY SASSI) mooring array on the
25 shelf in this particular location (the WAP). Further, this location is ideal given that it is

situated in the heart of the extensive (20 yr) gridded data set of the Palmer Long Term Ecological Research project (Pal LTER; Smith et al., 1995). This paper describes the array and findings.

2 Data

2.1 Study region

Most of the data for this study have been acquired in the LTER marine sampling grid shown in Fig. 1. The LTER project has collected shipboard data since 1991, including every January since 1993.

2.1.1 Physical setting

In this study region, as well as most of Western Antarctica, the ocean is a source of heat. The warmest water, characterized by a temperature maximum (T_{max}), is Upper Circumpolar Deep Water (UCDW) at $\geq 1.7\,°C$ as delivered to the WAP via the Antarctic Circumpolar Current (ACC). Martinson et al. (2008; hereafter MSISV08), using LTER data through 2004, show that on the WAP continental shelf, the heat content of the sub-surface water column (a 3 watermass mixture, dominated by UCDW) has increased. Webb (2011) documents a 50 yr exponential warming of UCDW in the ACC as it flows past Western Antarctica. As the predominant source of heat and nutrients, UCDW is the obvious water mass to focus on in gauging the slope-shelf interaction.

The LTER sampling grid overlays the broad continental shelf of the WAP at ~450 m in depth, running ~200 km in cross-shelf width and ~400 km along the WAP (recently extended another ~300 km further SW down the Peninsula). Sample sites are located on a grid system, delineated by "Grid Lines" that are 100 km apart and lie perpendicular to the average coastline. "Grid Stations" are spaced every 20 km along these grid lines across the shelf. Grid lines are labeled according to their position in the grid relative

Title Page

Abstract | Introduction

Conclusions | References

Tables | Figures

◄ | ►

◄ | ►

Back | Close

Full Screen / Esc

Printer-friendly Version

Interactive Discussion

to the original southern-most sample location; grid stations are labeled according to their cross-shelf distance from the average coast. Individual sites are identified as *ggg.sss*, where *ggg* is the grid line and *sss* is the grid station location. For example, site 300.100, the location of mooring #1, lies 100 km offshore on the grid line 300 km up the peninsula from the southern-most line of the grid, near Alexander Island with 000.000 at ~69.0° S, ~73.6° W; the 300.100 site is 60 km inshore of mooring #2 located at 300.160 and it is 100 km southwest (down the peninsula) of site 400.100, the location of mooring #3.

In the WAP, the southern boundary of the ACC, as defined by the southern-most presence of UCDW (Orsi et al., 1995), flows over the continental slope along the shelf break as it does throughout the entire SE Pacific region (Orsi et al., 1995; MSISV08) along the continental rim of the Amundsen-Bellingshausen Seas. This makes warm UCDW directly available to the continental shelf for easy ventilation to the atmosphere and glacial melt on the WAP shelf.

In this important respect, the West Antarctic continental shelf is unique in Antarctica for this spatially-extended proximity of the ACC and delivery of warm UCDW (Fig. 2).

2.1.2 Shipboard data

Ocean CTD data were collected every austral summer since 1993, as well as during multiple non-summer cruises (see MSISV08 for detailed description of these data). These data are available in the LTER database (http://pal.lternet.edu/data/), National Oceanographic Data Center (NODC) and in Martinson's LTER data page (http://www.ldeo.columbia.edu/~dgm/LTER.html), the latter also contains numerous derived products.

Hull-mounted ADCP data are also available from all LTER cruises. Those data were quality controlled, processed and released by *Teresa Chereskin* at Scripps Institution of Oceanography (http://pal.lternet.edu/data/ see "Other Palmer Data Resources"). We use the ADCP at-site data to assess upwelling contributions.

2.1.3 Moorings

Moorings were deployed (and subsequently recovered and redeployed) during the LTER summer (January) annual cruises. Mooring locations were guided by the extensive LTER CTD data as well as results from the 2001–2003 Southern Ocean Global Ecosystem Dynamics project (SO GLOBEC; Hofmann et al., 2004). The former reveal locations where the largest fraction of pure UCDW was distributed on the grid (presumably closest to the location where the UCDW enters the shelf). The latter show that UCDW enters Marguerite Trough (Klinck et al., 2004; Moffat et al., 2009). Consequently, we situate some of the thermistor moorings in this project to sample the region of high UCDW-fraction (Fig. 3) adjacent to Marguerite Trough.

Our Lamont thermistor moorings[1] contain fixed-depth SeaBird (SBE39) thermistors (some with pressure sensors; see Table 1 for details), sampling every 10 min (or in 2010, every 15 min). SBE39 thermistors possess an initial accuracy of 0.002 °C and resolution of 0.0001 °C. The vertical spacing and density of the thermistors on the string yield integrated heat content (Q) values that show an average bias of well under 0.1 %. Some moorings have current meters whose depths are given in Table 1. Their positions on the string allow us to sample the upper and lower water column, the depths of which are guided by shipboard ADCP data. Mooring data were de-tided using T_TIDE (Pawlowicz et al., 2002), which proves useful for velocities but does little to alter records of T. All velocity analyses use the de-tided values.

Mooring locations and years for which data were acquired are given in Table 1. Because of the continued success of moorings at 300.100, 300.160 and 400.100 and their ideal location relative to the location of highest fraction of pure UCDW, this study focuses primarily on the data from those moorings.

---

[1]Moorings designed by Lamont oceanographer Bruce Huber.

Transport of warm upper circumpolar deep water

D. G. Martinson

Title Page

Abstract	Introduction
Conclusions	References
Tables	Figures

|◄ | ►|

◄ | ►

Back | Close

Full Screen / Esc

Printer-friendly Version

Interactive Discussion

3 Analyses – mechanisms for moving UCDW onto the shelf

The ACC delivers UCDW to the WAP region and its southern edge flows along the shelf-slope break. Four mechanisms have been suggested for moving the UCDW from the ACC over the slope onto the shelf, the first two based on findings from the Southern Ocean GLOBEC:

1. eddies from the ACC shed onto the shelf;

2. entry into the canyons cutting across the shelf, and then overflow of the canyons filling the overlying shelf waters;

3. general upwelling;

4. shelf-wide flooding by episodic meanders of the ACC across the shelf.

3.1 Eddies

Moffat et al. (2009) document eddies migrating across the shelf adjacent to Marguerite Trough. We begin evaluation of this mechanism by examination of $Q(t)$ at mooring 300.100 – located on the northeastern wall of Marguerite Trough, 60 km inshore of the shelf-slope break where the southern margin of the ACC flows. The heat content of water available to melt ice is $Q = \int_{H}^{\text{wml}} \rho c_{\text{p}}[T(z) - T_{\text{f}}]dz$ where ρ is density, c_{p} heat capacity, T_{f} surface freezing point of seawater, and wml top of permanent pycnocline (which is the bottom of the winter mixed layer or base of the winter water, WW); $H = 415$ db and is chosen to be deep enough to represent all heat below wml and above the deepest sensor for all years on moorings 300.100 and 300.160[2].

---

[2]This differs from MSISV08 who integrate from wml down 300 db

3.1.1 Qualitative inspection

$Q(t)$ shows considerable high-frequency variability that we treat as noise (Fig. 4). We remove the noise by using the first mode of a Karhunen-Loéve transform, performed with the number of modes restricted to $m = 19$. This forces all of the variance to be
5 described by no more than 19 modes, though for these series, most of the variance is contained in mode 1 over a broad range of m values. We prefer this to a more standard filter (e.g. some form of convolution) since there is no phase shift or temporal smearing of the series, and the method is data-adaptive. The first mode is used as the smoothed version of $Q(t)$ upon which we perform most of our analyses.
10 Inspection of the smoothed Q series at 300.100 for each year shows frequent episodic short-lived increases in Q, or "Q-events" (Fig. 5). Notable is the fact that the rate of Q increase (dQ/dt) appears to be remarkably similar in most cases. One explanation for this is that comparable-sized warm-core eddies move past the mooring site following the same path due to bathymetric tracking.
15 More telling is the fact that nearly every Q-event contains water well above 1.7 °C, (sometimes as high as 2 °C; Figs. 5 and 6). The only water within the LTER sampling grid that occurs at temperatures this high is UCDW as it appears in its unmodified form within the ACC over the continental slope as delivered to the WAP. Nowhere on the continental shelf, except in the core of these events, is water this warm encountered
20 (MSISV08).
The $T_{\max}$ series of Fig. 5 and T-sections of Fig. 6 highlight the rapid temporal variability of the water column at 300.100, further justifying our need to smooth the Q-series and focus on the major "long" lasting features (i.e., Q-events).

Bathymetry tracking

25 Besides the consistent dQ/dt and waters with $T_{\max} \geq 1.7$ °C arguing for movement of comparable-sized warm-core eddies, other features point to this conclusion. Mooring

Title Page

Abstract | Introduction

Conclusions | References

Tables | Figures

◄ | ►

◄ | ►

Back | Close

Full Screen / Esc

Printer-friendly Version

Interactive Discussion

#5 (300.120, Fig. 1), also on the northeast wall, is 20 km offshore of mooring #1 (300.100), and the Q records at these 2 locations are well correlated ($r^2 > 50\%$) with a lag time of 2.25 days for unsmoothed series and 2.75 days for the smoothed Q series. This equates to drift rates along the northeastern wall of $\sim$0.1 m s^{-1}, consistent with velocities measured by the Schofield LTER glider fleet (personal communication). Finally, observed current velocities at the 300.100 mooring, if projected as trajectories forward, show a drift following the canyon wall's fork to the east (Fig. 7), again consistent with the currents transporting eddies tracking the bathymetry.

3.1.2 Quantitative analysis

We combine approaches similar to those of Moffat et al. (2009) and Lilly and Rhines (2002) to quantify the signature of eddies in our observations, focusing on mooring #1 (300.100). We identify eddies by examining the velocity data recorded (V_{obs}) in the 280 m current meter (close to the center of the lower layer warm water boluses seen in Fig. 6) and the 4 closest (in depth) T-sensors. These records are de-tided and smoothed by a cosine-Lanczos filter centered at 24 h to remove non-tidal high frequency fluctuations. We define a background drift V_{bg} (advecting the eddies) as the first mode of a complex singular spectrum analysis with 121 modes, providing a series that is everything that is not the eddy rotation itself (a method we are satisfied with based on the clean eddy rotations we detect in the residuals). The eddy velocity, $V_e = V_{obs} - V_{bg}$, is then rotated via a phasor, $e^{-i\varphi}$, where φ is the argument of complex V_{bg}. This rotates V_e to be relative to the direction of the background flow (V_{bg}), most easily allowing identification of rotation independent of the background drift. Assuming a rankine vortex model, rotation of the eddy core is identified as two extrema of opposite sign in the *cross-stream* component of V_e occurring simultaneously with a fixed-sign, symmetric magnitude reversal in the *along-stream* component of V_e. The two extrema mark the moments of maximum flow perpendicular to V_{bg} and therefore the extent of the eddy core.

Transport of warm upper circumpolar deep water

D. G. Martinson

Since Fig. 6 suggests that Q-events are approximately centered about peaks in T, we find all occasions where T_{max} goes above 1.7 °C and then descends by at least 0.1 °C to below 1.7 °C. Specifically, for each such occasion we define t_{Ti} (the time where T_{max} begins increasing towards 1.7 °C) and t_{Te} (the time after t_{Ti} where T_{max} stops decreasing and is below 1.7 °C and is at least 0.1 °C below the previous extremum in T_{max}). The constraint in the magnitude of ΔT_{max} is to avoid artificially cutting off a single event. Some of the Q-events of the previous section span more than one such peak in T_{max}.

While the peaks in T_{max} are found in an automated manner, the velocity records are inspected manually because there can be (though rarely so) more than one eddy within a single peak in T_{max}. Within each peak in T_{max}, augmented by 24 h in both directions – that is, $\Delta t_T = [t_{Ti} - 24, t_{Te} + 24]$ – we examine V_e for the signs of eddy rotation described above: (1) a point where V_e moves perpendicular to the background flow, defining the initial eddy presence at the mooring (t_{ei}), and (2) that time where V_e is again perpendicular to the background flow, but in the opposite direction, defining the end of the eddy presence at the mooring (t_{ee}). To do so, *all* extrema in the cross-stream component of V_e within Δt_T are found and the eddy (or eddies) temporal extent(s), $\Delta t_v = t_{ee} - t_{ei}$, are chosen from this subset of points. A progressive vector diagram for the eddy within Δt_T, color-coded by T_{max}, is examined to determine which of the extrema in the cross-stream eddy velocity are the proper ones to define the bounds of the eddy chord. An eddy should manifest as approximately U-shaped with a warm core. An example of the implementation of the method is shown in Fig. 8.

Eddies are drifting at the background velocity, V_{bg}, past the mooring, thus an estimate of eddy diameter (actually, chord length) is $L_e = V_{bg} \Delta t_v$. Since we are seeking extrema in the cross-stream component of V_e, we are effectively deriving metrics of the eddy core as opposed to the entire eddy. In some cases we are unable to cleanly detect the velocity signature of an eddy though this does not mean that there is not an eddy present within a given Δt_T, even if not identified here.

Transport of warm upper circumpolar deep water

D. G. Martinson

Bathymetric tracking is consistent with a formation location of eddies at the slope-shelf break at location 300.160 (mooring #2). Klinck et al. (2004) show that where Marguerite Trough intersects the shelf break, the shelf break itself projects to the west into the oncoming ACC, driving the ACC into the northeastern wall of the Trough gen-

5 erating a pressure head that drives UCDW into the Trough. This disturbance is likely to also generate eddies. If the eddies observed at mooring #1 (300.100) are generated at 300.160 (where mooring #2 is), they would likely have the same radius. Likewise, if they were drifting with the average current, tracking bathymetry (in this case topography along the northeastern wall), they would have drifted over mooring 300.100 at a

10 similar rate, giving a similar dQ/dt – as observed.

Estimates for all eddy diameters yield Gaussian-like distributions (skewed toward larger L_e, as expected for chords approaching the true diameter). Table 2 presents the number of eddies per year at mooring 300.100 as well as their diameters' (in km) mean, median and standard error about the mean for all 3 yr.

15 We examine 23 CTD casts (since 1993) at 300.160 (within a 4×4 km square, centered at 300.160), where we believe the eddies are generated. The first internal Rossby radius, $L_R = [g' h_1 h_2/(h_1 + h_2)]^{1/2}/f$, for a two-layer system with layer thicknesses $h_1 = 170$ m and $h_2 = 320$ m – a good approximation for this Antarctic water column – gives $L_R = 4.8 \pm 0.08$ km. The eddies at mooring #1 (300.100) have yearly median di-

20 ameters of 6.4–10 km. Unless the eddies pass perfectly centered over the mooring, our "diameter" will actually be a chord length, and thus less than the true diameter. The eddy characteristics are consistent with L_R at the suspected formation site (300.160).

The Q-series at mooring #3 (400.100) shows considerably fewer eddy signatures. Their temperature core is slightly less than that of the events at 300.100. Eddies at that

25 site are not investigated since this study focuses on how the UCDW enters the shelf from the ACC waters over the slope. At mooring #4 (460.046), T_{max} never exceeded 1.4 °C and at mooring #6 (230.−035), T_{max} was consistently less than 1 °C, so eddies at those sites are not transporting pure (as delivered to WAP via the ACC) UCDW.

3.2 Overflow of canyons

Klinck et al. (2004) show from SO GLOBEC data (2001–2003) that UCDW enters Marguerite Trough (the major canyon crossing the WAP shelf). If this water then overflows the trough onto the nominal shelf floor, we would expect to see a signal of ocean heat increasing from the bottom of the mooring upward. Mooring #1 (300.100) is well positioned to test this mechanism, being adjacent to the northeastern wall of Marguerite Trough. We carefully examined *all* of the 1 h-averaged temperature profiles for the 3 yr of mooring data adjacent to the Marguerite Trough and observed this behavior only once (and even that was equivocal), suggesting that this mechanism is not active.

3.3 Upwelling

MSISV08 showed that the increase in ocean heat content on the WAP shelf (using the 1993–2004 LTER January shipboard CTD data) showed a positive covariation with the depth of the pycnocline: elevated pycnoclines (interpreted as upwelling) correlated to increased ocean heat to the extent that 87 % of the variance of ocean heat could be ascribed to upwelling.

We examined the shipboard ADCP profiles at 300.100 to isolate those times when mass balance was approximately achieved, to compute an upwelling heat flux. For example, in 2007, we see water over the upper 170 m of the water column moving offshore at an average speed of $0.015 \, \mathrm{m \, s^{-1}}$; the 300 m water column below this upper layer was moving onshore at $0.0076 \, \mathrm{m \, s^{-1}}$. Assuming these are constant over the 4×10^5 m length of the LTER sample grid (consistent with a SLOCUM glider run in 2007), suggests 1 Sverdrup ($10^6 \, \mathrm{m^3 \, s^{-1}}$) offshore Ekman surface flow balanced by 0.9 Sv onshore flow (upwelling). The temperature contrast of $1.2 \, ^\circ \mathrm{C}$ between the two layers gives a reasonable upwelling heat flux of $69 \, \mathrm{W m^{-2}}$. However, the fluxes were unrealistic for nearly all other cases, suggesting that we could not use this method to better quantify the fraction of warm water contribution over a year by upwelling.

We also know that the correspondence between the elevated pycnocline and Q may just as well describe eddy boluses passing the site (Fig. 6), so this mechanism described in MSISV08 cannot differentiate the 87 % described Q variance due to upwelling from that due to eddies.

3.4 Shelf-wide flooding

If shelf-wide flooding events are a mechanism moving warm ACC waters onto the shelf, we would expect to see them as lagged coherent events in $Q(t)$ across the entire mooring array. We do see lagged correlation between mooring #5 and #1, 20 km apart, but have shown that the correlative features are eddies. We do not see correlation of Q across the complete mooring array as expected for a shelf-wide event, thus eliminating this mechanism.

4 Conclusions

The evidence presented here strongly favors eddies as the mechanism for delivering warm (UCDW) water to the continental shelf. The presence of UCDW-core eddies is consistent with the conclusions of Moffat et al. (2009).

Distinct jumps in ocean heat content (Q-events) at mid-shelf mooring #1 (300.100): (1) show remarkably consistent dQ/dt over three years of observations, suggesting bathymetric steering of similar sized eddies over the mooring site, (2) coincide with warm water boluses that show distinct rotation (usually anticyclonic) with the core water warmer than 1.7 °C, which is found only in UCDW within the ACC at the shelf break where UCDW is delivered via the ACC, (3) are related to eddies, with the larger chord lengths (closer to a true diameter) consistent with the Rossby radius at the shelf break where the eddies were presumably formed.

These features, along with projected trajectories at 300.100 suggesting bathymetric steering following the canyon wall still on the eastern branch of Marguerite Trough,

allow a reasonable estimate of the eddy generation site: the warm core suggests the ACC over the slope and bathymetric tracking suggests where the NE wall of Marguerite Trough intersects the shelf break at our site 300.160 (mooring #2). That location is consistent with Klinck et al. (2004) as a site where the shelf protrudes into the oncoming ACC driving water into the trough, but also likely generating eddies with a cross-shelf expression guiding the onshore current advecting them past moorings 300.120 and 300.100 (thus similar dQ/dt, and eddy chord lengths).

We do not know the rate at which the warm temperature core of the eddies is dissipated to the surrounding water, but will test this in the near future using our LTER (Schofield) SLOCUM glider fleet that is capable of tracking eddies. In general, there appears to be approximately 3 eddies per month (though there are fewer observed in autumn).

References

Cook, A. J., Fox, A. J., Vaughan, D. G., and Ferrigno, J. C.: Retreating glacial fronts on the Antarctic Peninsula over the past half-century, Science, 308, 541–544, 2005.

Hofmann, E. E., Wiebe, P., Costa, P., and Torres, J. J.: An overview of the southern ocean global ocean ecosystems dynamics program, Deep Sea Res. Part II, 51, 1921–1924, 2004.

Klinck, J. M., Hofmann, E. E., Beardsley, R. C., Salihoglu, B., and Howard, S.: Water-mass properties and circulation on the west Antarctic peninsula continental shelf in austral fall and winter 2001, Deep Sea Res. Part II, 51, 1925–1946, 2004.

Lilly, J. M. and Rhines, P. B.: Coherent eddies in the Labrador Sea observed from a mooring, J. Phys. Oce., 32, 585–598, 2002.

Martinson, D. G., Stammerjohn, S. E., Iannuzzi, R. A., Smith, R. C., and Vernet, M.: Western Antarctic Peninsula physical oceanography and spatio-temporal variability, Deep Sea Res. Part II, 55, 1964–1987, 2008.

Moffat, C., Owens, B., and Beardsley, R. C.: On the characteristics of Circumpolar Deep Water intrusions to the west Antarctic Peninsula Continental Shelf, J. Geophys. Res., 114, C05017, 1–16, 2009.

Orsi, A. H., Whitworth, T., and Nowlin, W. D.: On the meridional extent and fronts of the Antarctic Circumpolar Current, Deep Sea Res., Part I, 42, 641–673, 1995.

Pawlowicz, R., Beardsley, B., and Lentz, S.: Classical tidal harmonic analysis including error estimates in MATLAB using T_TIDE, Computers and Geosciences, 28, 929–937, 2002.

Rignot, E., Bamber, J. L., van den Broeke, M. R., Davis, C., Li, Y., van de Berg, W. J., and van Meijgaard, E.: Recent Antarctic ice mass loss from radar interferometry and regional climate modeling, Nat.Geosci., 1, 106–110, 2008.

Smith, R. C., Baker, K. S., Fraser, W. R., Hofmann, E. E., Karl, D. M., Klinck, J. M., Quetin, L. B., Prézelin, B. B., Ross, R. M., Trivelpiece, W. Z., and Vernet, M.: The Palmer Pal LTER: A long-term ecological research program at Palmer Station, Antarctica, Oceanography, 8, 77–86, 1995.

Vaughan, D. G.: How does the Antarctic ice sheet affect sea level rise?, Science, 308, 1877–1878, 2005.

Webb, L.: Deep waters melting West Antarctica Ice Sheet Fringe mirror global ocean exponential warming, MA thesis, Columbia University, 2011.

Title Page

Abstract | Introduction

Conclusions | References

Tables | Figures

◀ | ▶

◀ | ▶

Back | Close

Full Screen / Esc

Printer-friendly Version

Interactive Discussion

Table 1. Mooring locations, years at location and sensor suite. Mooring numbers agree with numbered circles in sample grid of Fig. 1. Current meter abbreviations are: S4: InterOcean, and AE: JFE ALEC Electronics – both are electromagnetic current meters.

Mooring Number	Location/ Name	Years w/Data	# of T Depths	# of T with Pr	Current Meter 1 Depth	Current Meter 2 Depth
1	300.100	2007	11	5	S4 $\sim$ 280 db	S4 $\sim$ 84 db
		2008	11	5	S4 $\sim$ 279 db	–
		2010	15	7	AE $\sim$ 189 db	AE $\sim$ 288 db
2	300.160	2008	17	9	S4 $\sim$ 323 db	–
		2009	17	8	S4 $\sim$ 321 db	–
		2010	17	8	AE $\sim$ 188 db	–
3	400.100	2008	17	8	S4 $\sim$ 290 db	–
		2009	17	9	S4 $\sim$ 271 db	–
		2010	14	4	AE $\sim$ 233 db	AE $\sim$ 89 db
4	460.046	2008	13	6	S4 $\sim$ 315 db	–
5	300.120	2010	17	8	–	–
6	230.$-$035	2008	9	5	–	–
		2009	9	5	–	–

Table 2. Number of eddies per year at 300.100, and their size.

Year	Number eddies	Mean diameter ± standard error (km)	Median diameter (km)
2007	35	8.2 ± 1.0	7.6
2008	40	9.9 ± 1.4	6.4
2010	37	10.2 ± 0.9	9.9
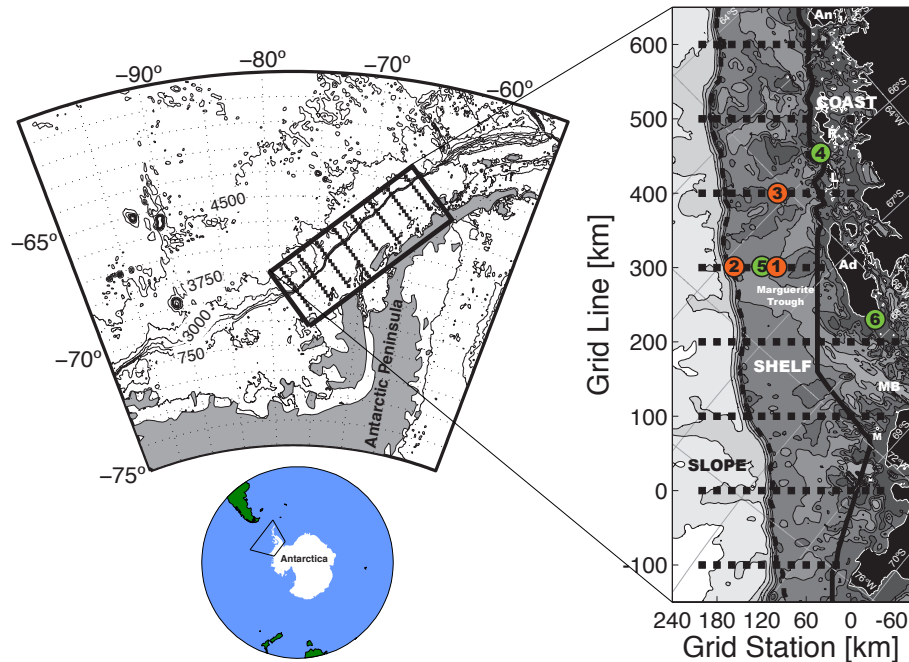
Fig. 1. Location of LTER marine sampling grid from which data for this study have been acquired. Shipboard (CTD) sampling locations shown as solid squares. Numbered circles in sample grid (right panel) show the various mooring locations during the years of data included in this study (2007–2010); Table 1 lists the specific mooring locations for each year. Mooring #1 was deployed in 2007 as part of the LTER project. All others in 2008 and beyond as part of the IPY SASSI project (never more than five moorings deployed in any one year). Gold colored mooring sites are most consistently occupied and primary focus of this study, green ones less so. Marguerite Trough (labeled) cuts across the center of the shelf into Marguerite Bay (labeled: MB). Grid bathymetry shaded between contours every 150 m from 200 m until 750, and then at 750 m intervals until 3750.

Title Page

Abstract | Introduction

Conclusions | References

Tables | Figures

|◄ | ►|

◄ | ►

Back | Close

Full Screen / Esc

Printer-friendly Version

Interactive Discussion
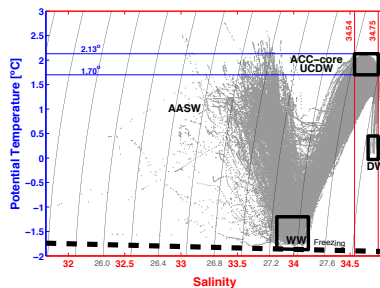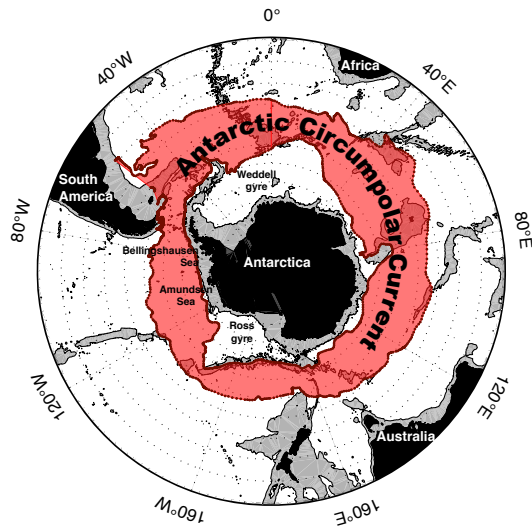
Fig. 2. Location of climatological ACC, transporting warm UCDW. The ACC flows along the slope-shelf break for the entire Western Antarctic. Bathymetry shallower than 3 km is shaded. Lower panel showing primary water masses in LTER sampling grid (from *MSISV08*), UCDW is warmest water in water column, occasionally exceeded in temperature by the summer surface layer (AASW).
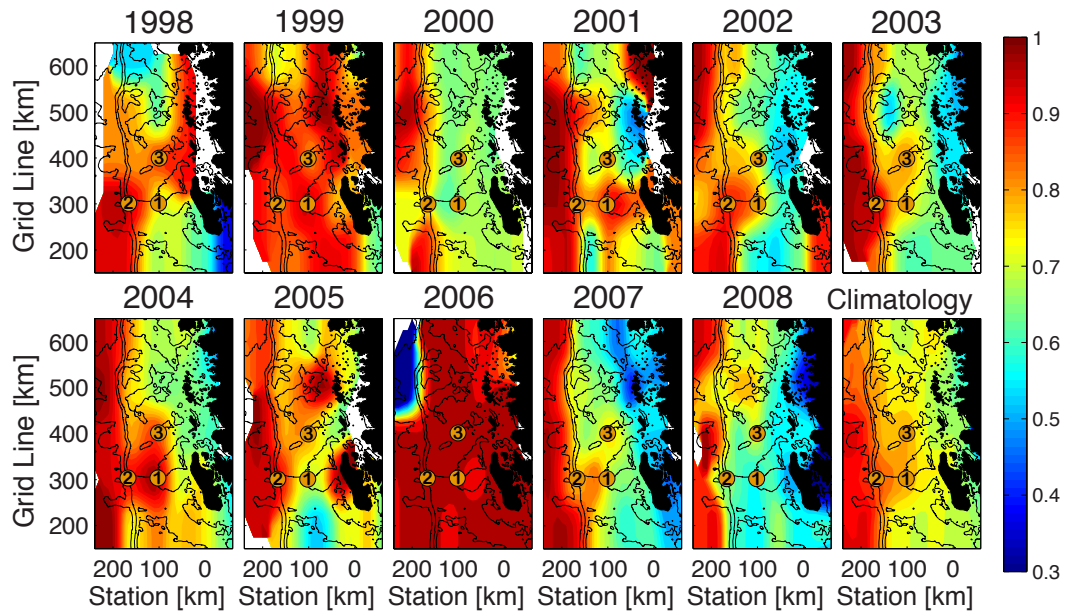
Fig. 3. Fraction of pure UCDW in the LTER grid as a function of year; location of mooring sites 1–3 indicated. Bathymetry contours at 450, 1500 and 3000 m.
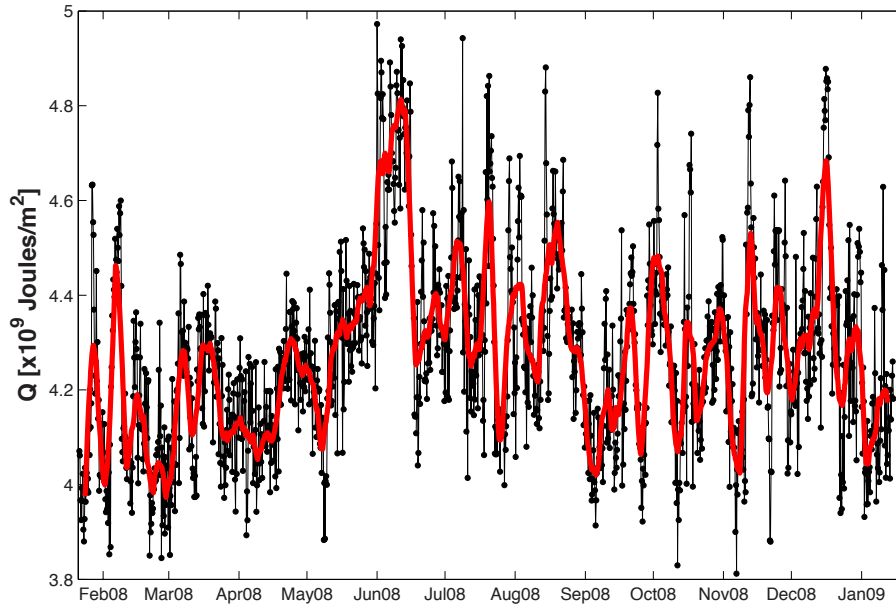
Fig. 4. Time series of Q (dots with black line) for mooring 300.100 in 2008 with the gravest mode of the Karhunen-Loéve transform as a filter (red) being the smoothed version used for the analyses.
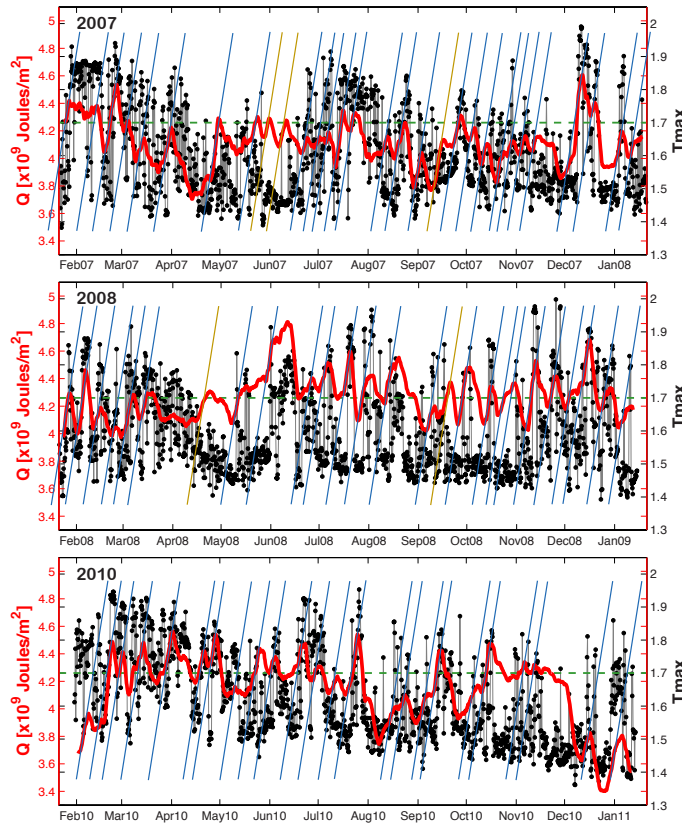
Fig. 5. For the mooring at 300.100, the gravest mode of Q (solid red line) overlaying T_{max} (black line with dots). Nearly every Q-event shows a core T_{max} greater than 1.7 °C (pure UCDW). Blue slanted lines (*all* of the same slope) show similar dQ/dt for each event. Gold slanted lines (same slope as blue lines) show rare events not coincident with $T_{max} \geq 1.7$ °C.
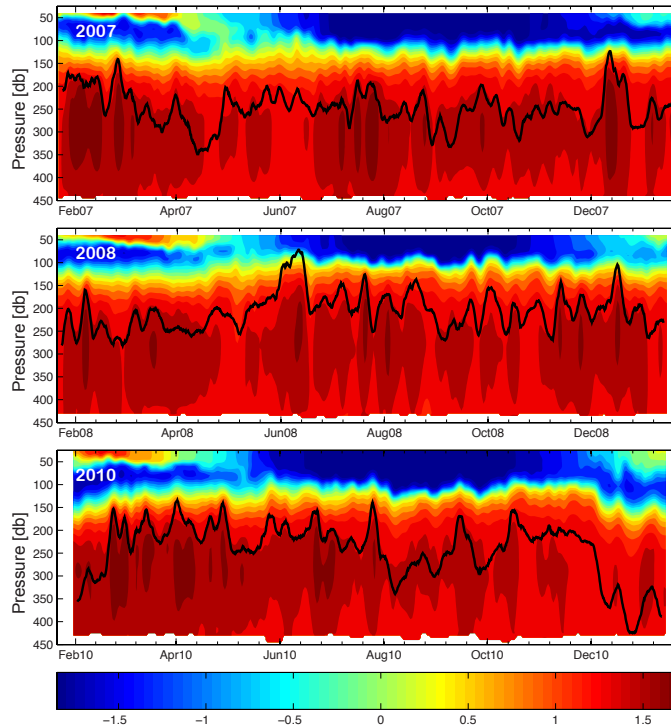
Fig. 6. For the mooring at 300.100, T as a function of depth and time, with Q-series overlain (black line) to show the relationship between T and Q-events. Q-events clearly coincide with warm (red) deep anticyclonic boluses. Arrows on right ordinate show depths of T sensors. Color bar show temperature scale.
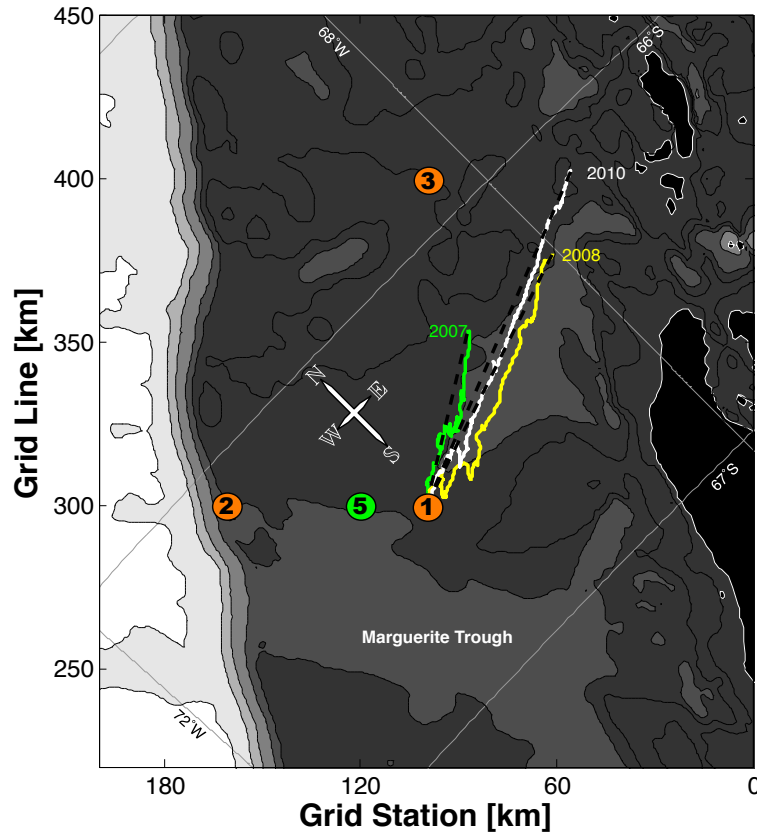
Fig. 7. Progressive vector diagram for the velocities at mooring site #1 (300.100). If the flow observed at the mooring at all time steps was extended into a Lagrangian trajectory, the flow would track the northern wall of the Marguerite Trough's Eastern fork (i.e. track the same bathymetry from the slope-shelf break). The vector lengths are scaled so as to fit onto the image.
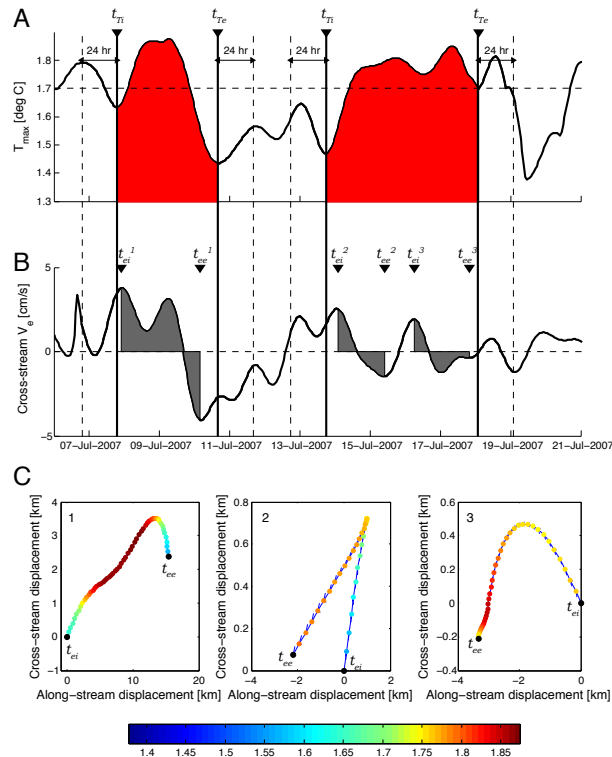
Fig. 8. Example of detection scheme for two detected T_{max} peaks – not the cleanest examples in the records, but rather a case of one eddy followed by the much more rare case of two eddies. A. Time series of T_{max}, showing the search windows $\Delta t_T = [t_{Ti} - 24\,h, t_{Te} + 24\,h]$ for two detected peaks in T_{max}. B. The cross-stream eddy velocity over the same time intervals with the chosen bounds for the ith eddy, denoted by $\Delta t_v^i = [t_{ei}^i, t_{ee}^i]$, within corresponding Δt_T. C. Progressive vector diagrams for the eddy velocity of the three eddies found in (B), summed over Δt_v^i and color coded by T_{max}.

Full Screen / Esc

Printer-friendly Version

Interactive Discussion